URSI AP-RASC, Sydney, Australia, 17 – 22 August 2025

Automatic Detection of Radio Bursts with Frequency Integral Spectrum and Hough Transforms

Rui Tang [(1)], Baolin Hou [(1)], Mingwei Qin* [(1)], Jingsong Ping* [(1,2,3)], Zamri Bin Zainal Abidin [(4)], Yun Deng [(1)], and Fukang Zhou [(1)]
(1) School of Information Engineering, Southwest University of Science and Technology, Mianyang 621010, China;
(2) National Astronomical Observatories, Chinese Academy of Sciences, Beijing 100101, China;
(3) University of Chinese Academy of Sciences, No.1 Yanqihu East Rd, Huairou District, Beijing, PR China, 101408;
(4) Department of Physics, Lingkungan Budi, University Malaya, 50603, Kuala Lumpu;

Abstract

In this study, we propose an automated method that combines frequency integral spectrum analysis with the Hough transform to identify outburst events in the solar radio spectrum. By leveraging the distinct characteristics of various radio events, we effectively differentiate between type II and type III events in the automatic detection results. Furthermore, we eliminate misclassified WBI, which enhances the validity and accuracy of the detection outcomes. This work may benefit the study of establishing a crucial foundation for space weather warnings and heliophysical research.

1. Introduction

A primary driver of Sun-Earth space weather is the intense activity of the sun, particularly the solar flares and coronal mass ejections (CMEs) [1]. These phenomena are often accompanied by solar radio bursts at various frequencies. Based on their spectral characteristics, radio bursts are classified into five types: I, II, III, IV, and V [2]. When electromagnetic radiation, energetic particles, and plasma from these solar eruption events, along with the magnetic fields they carry, propagate toward the Earth, they can have significant effects on human activities. For instance, energetic particles and shock waves in the near-Earth space environment can damage satellites and probes; disturbances in the ionosphere can disrupt oceanic communications [3]; energetic electrons injected into the magnetosphere can excite electromagnetic radiation in the auroral region, thereby interfering with the normal operation of communication systems; and the coupling of high-speed solar wind or magnetic clouds with the Earth's magnetic field can trigger geomagnetic disturbances, potentially damaging terrestrial power grid equipment [4].

To enhance our understanding of solar activity, research organizations worldwide are continuously investing in advanced observational equipment to collect solar activity data with high temporal, spatial, and frequency resolution. Currently, over 150 observatories are operational globally, facilitating all-weather monitoring of the sun. These stations generate vast amounts of data, presenting a significant challenge for data analysis experts. At present, global monitoring of the solar radio spectrum still relies heavily on traditional manual detection methods. This reliance creates an unmet need for real-time detection and response to solar outburst events. Furthermore, the complexity of radio data exacerbates the difficulty of identifying these outbursts. The duration of solar radio bursts varies considerably, and some of these events are transient, making it challenging for traditional manual analyses to effectively capture these fleeting phenomena. Additionally, the faintness of the radio signals increases the risk of confusion with background noise, which may lead to misclassification or omission of outburst events [5]. In light of these challenges, the development of automated event selection and feature extraction methods is crucial for scientific research.

2. Methodology

In this study, solar radio dynamic spectral data were collected by the Xinjiang Astronomical Observatory, Chinese Academy of Sciences, and Qitai Observatory[6]. The observatory consists of eight dual-polarized, log-periodic antennas, each measuring 10 meters in length, covering a wavelength range of 3 to 30 meters and a frequency range of 0 to 100 MHz. The radio receiver is a self-developed, eight-channel radio analyzer capable of storing acquired data in binary format (.bin files) on a disk array, organized by date. The dataset includes both horizontally and vertically polarized components, with a time resolution of 20 milliseconds and a frequency resolution of 24 kHz. For this study, data collected between 2023 and 2024 were selected for analysis.

The automatic detection algorithm presented in this article is based on the frequency integral spectrum and the Hough transform. The algorithm begins with interference suppression in the radio spectrum through data preprocessing. Next, the interference-suppressed spectrum is integrated along the frequency axis to generate a frequency integral spectrum, which serves as the foundation for identifying potential burst events. To enhance detection accuracy, the algorithm employs an adaptive thresholding technique similar to the constant false alarm rate (CFAR) method in the frequency integral spectrum. Then, because the preliminary detection results cannot differentiate between Type II and Type III events, and due to potential interference, the algorithm performs binary processing based on the spectral line flow of the preliminary detection results and executes the Hough transform. Since radio bursts exhibit different frequency drift characteristics in the spectrum, this information can be utilized to effectively classify these events. The flow chart of the algorithm is shown in Figure 1.

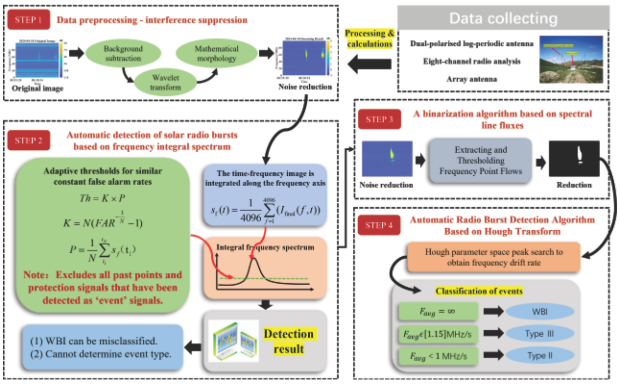

Figure 1. Flow of the Automatic Radio Burst Detection Algorithm Based on frequency integral spectrum and Hough Transform.

3. Event detection

Given a time-frequency dynamic spectrum $I_{final}(f,t)$ after interference suppression, the frequency-integrated spectrum is obtained by integrating the dynamic spectrum along the frequency axis. The equipment used in this study collects spectrum data with 4,096 frequency channels. The integration process is expressed in Equation (1).

$$s_f(t) = \frac{1}{4096}\sum_{f=1}^{4096}(I_{final}(f,t)) \quad (1)$$

The selection of an appropriate threshold is crucial when detecting events in the frequency integral spectrum. Setting the threshold too low can lead to a high number of false alarms, potentially obscuring genuine solar events. On the other hand, setting the threshold too high reduces false alarms but limits detection to only major solar events, resulting in the omission of many low-energy solar events. A common approach to addressing the false alarm problem is the cell CFAR detector. In this study, an adaptive threshold, denoted as 'Th' is applied to the frequency integral spectrum $s_f(t)$. The threshold 'Th' is determined using the calculation shown in Equation (2).

$$Th = K \times P \quad (2)$$

Where P corresponds to the average power of the background noise within the referenced time window N. K is a threshold factor that is adjusted immediately to maintain a CFAR. The average power P is calculated in Equation (3).

$$P = \frac{1}{N}\sum_{t_1}^{t_N} s_f(t_i) \quad (3)$$

Where N is the selected window length and $s_f(t)$ is the spectral signal in the window after interference suppression. The threshold factor K can be calculated from Equation (4).

$$K = N(FAR^{-\frac{1}{N}} - 1) \quad (4)$$

Where N is the selected window length, and FAR is the false alarm rate.

Since the assumed independent identically distributed Gaussian model does not match the actual data model, in practice, instead of using the K-value computed by the above formula, one usually adopts the value corresponding to the target false alarm rate, which is obtained through actual training and is called the 'experimental' value. In addition, in order to prevent energy leakage, all past points and protection signals that have been detected as 'event' signals in the reference window are eliminated in this paper. Based on the detection principle outlined above, we obtained the results shown in Figure 2. It is evident from the figure that the threshold line effectively differentiates between background noise and actual events, successfully detecting two events. For Event 2, the orange line indicates that this event appears three times with values exceeding the threshold. However, this actually represents a single event. Consequently, when the distance between two labeled events is less than the minimum distance of 3 seconds—calculated based on the resolution of the radio spectrometer and the averaging time of the solar events—the two signals are merged into one event. Conversely, if the distance between any group of detected solar radio events and another group exceeds the minimum distance of 3 seconds, the signals from that group are classified as a new event.

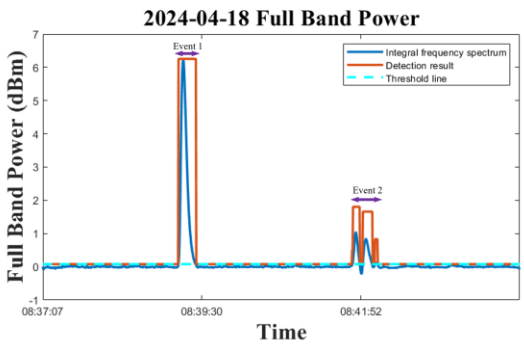

Figure 2. Results of radio burst detection based on frequency integral spectrum.

Through the radio burst detection method based on the frequency integral spectrum, we can determine whether there is a radio event in the solar radio spectrum signal, but it is not yet possible to determine the type of the event. For this reason, a detection algorithm based on the Hough transform is used in this paper to identify type II and type III radio burst events detected based on the frequency integral spectrum. In addition, frequency integral spectrum analyses may reveal misleading additional peaks produced by WBI that resemble the peaks of genuine solar radio events. This similarity increases the risk of misidentifying the interference as a legitimate radio event. As shown in Figure 3, we selected a section of the solar radio spectrum from 29 July 2024, where the red arrow marks the location of the solar radio event and the green arrow indicates the WBI. This interference resulted in inaccurate detection results. To ensure the accuracy and validity of the results, effective measures must be taken to identify and reject these WBI.

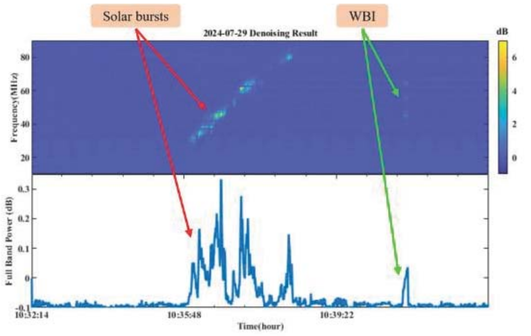

Figure 3. Solar radio spectrum after interference suppression. The red line represents the solar radio signal, and the green line represents WBI.

4. Event classification principle

Before performing the Hough transform, it is essential to binarize the image. Without binarization, the Hough transform considers every pixel in the grayscale image as a potential edge point, which significantly increases computational demands and the likelihood of false detections. Therefore, binarization is a critical step in executing the Hough transform. Following binary processing based on spectral line flow, the Hough transform is employed to identify solar radio burst events. For solar radio burst events, we can distinguish these occurrences by identifying the straight lines typically observed in the radio spectrum. The fundamental principle of Hough line detection is rooted in the duality of points and lines: every straight line in the image space corresponds to a point in the Hough parameter space. By locating the peaks in the Hough parameter space, we can ascertain the parameters that characterize the straight-line features of the radio burst, allowing us to locate and identify the events in the original image. In this paper, we extract the coordinates of the endpoints of the line segments to directly obtain the onset frequency, cutoff frequency, onset time, and cutoff time of the burst event from the detected red line segments. Additionally, the average drift rate of the event can be calculated using Equations (5):

$$F_{avg} = \frac{F_{stop} - F_{start}}{t_{stop} - t_{start}} \tag{5}$$

If the average frequency drift rate is negative, it indicates that the event is shifting from high to low frequencies. Based on our experience with the data from the Xinjiang Observatory's Qitai Observatory that we utilized:

(1) The drift rate of Type III radio bursts ranges from approximately 1 to 15 MHz/s.
(2) The frequency drift rate of type II radio bursts is typically less than 1 MHz/s.
(3) The frequency drift rate of WBI is infinite.

Therefore, matching the average drift rates obtained from the detection results of the Hough transform and successfully classifying type II and type III events can also help eliminate the misclassification of WBI.

5. Event classification result

In this study, we analyze observational data collected on July 29, 2024, at the Qitai Observatory of the Xinjiang Observatory, part of the Chinese Academy of Sciences, using an automated extraction algorithm. The objective of this process is to identify Type II radio burst events and accurately extract the key parameters associated with these events. Figure 5 shows the detection results of Type II radio events and WBI. We find that the Hough transform effectively extracts the parameter information of the event through the red line segments.

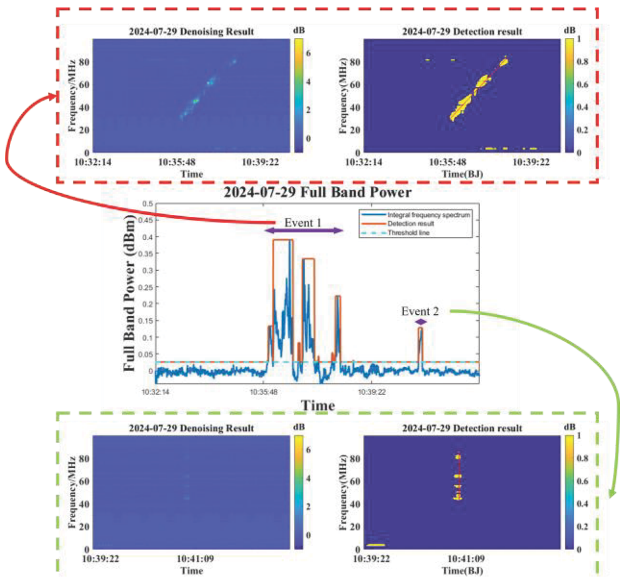

Figure 4. Solar radio spectrum detections on 29 July 2024 at around 10:00 pm. The top image shows the detected solar type II event, the middle shows the detection results based on the frequency integral spectrum, and the bottom shows the detected broadband interference.

In addition, parameters extracted from the Hough transform show that the mean drift rate of Event 1 is 0.41457 MHz/s, which is consistent with the frequency drift characteristics of our Type II radio events; thus, it can be determined to be a Type II radio outburst. However, the average drift rate of Event 2 is ∞, which indicates that the event does not have frequency drift characteristics, and thus it is judged to be a broadband disturbance. The results of this detection are eliminated from the final results, thus increasing the accuracy of the detection. For the detection of Type III events and parameter extraction, we employ the same approach, with the exception that we utilize an average frequency drift rate that meets the criteria for identifying Type III events when differentiating between various events.

5.2 Performance Evaluation

Since our goal is to develop an automated detection method, we define an evaluation scheme based on this. Indeed, the concepts of TP (True case), TN (True negative example), FP (False positive), and FN (False negative) are very standard and widely used in detection and classification theory. In this study, we use this assessment scheme to compare the duration of events labeled by experts (representing real situations) with the duration of events detected by our method. Figure 7 shows the results of solar event detection and the evaluation protocol employed in our simulations. As depicted in the figure, correctly detected solar events are time periods identified as solar radio events by both the expert's manual labeling and the method proposed in this paper. Conversely, incorrectly detected solar events are time periods that the expert does not recognize as genuine solar events but are classified as such by this method. Based on the definitions of these evaluation criteria, it is evident that high sensitivity and accuracy can only be achieved if the start and end times of the events detected by the system align with the expert labeling. Utilizing the performance evaluation methods outlined above, the sensitivity, precision, and accuracy were calculated to be as high as 97.2%, 89%, and 93.1%, respectively, for 10 events collected in 2024 at the Xinjiang Astronomical Observatory of the Chinese Academy of Sciences.

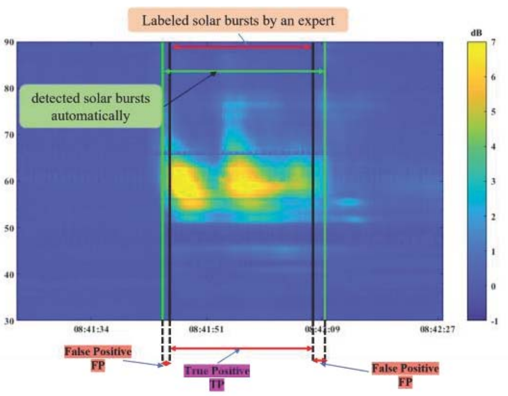

Figure 5. Comparison of automatic and manual test results.

6. Discussion: Future Context

The effective detection of solar radio events is essential for a comprehensive study of solar activity and space weather forecasting. Here, we introduce and propose an innovative method that combines frequency integral spectrum analysis with the Hough transform. Through interference suppression preprocessing, frequency integral spectrum detection, binarization, and the Hough transform, we can effectively detect solar radio events, classify type II and type III events, and eliminate misdiagnosed WBI. However, in our classification of radio events, we have only identified type II and type III events. In the future, we need to further investigate the characteristics of other event types and develop effective identification methods for them.

7. Acknowledgements

This research was funded by the National Key Research and Development Program's intergovernmental International Science and Technology Innovation cooperation project titled "Space Remote Sensing and Radio Astronomy Observation of Space Weather in Low and Middle Latitudes" (project number: 2022YFE0140000). Email: jsping@bao.ac.cn

References

[1] J. A. Yashan Hettiarachchi, Chandana Jayaratne, Sasani Jayawardhana, Christian Monstein, "The analysis of type II and type III solar radio bursts: GUI for the e-CALLISTO data," New Astronomy, vol. 109, p. 102194, 2024, doi: 10.1016/j.newast.2024.102194.

[2] F. Minta, S. Nozawa, K. Kozarev, A. Elsaid, and A. Mahrous, "Solar radio bursts observations by Egypt-Alexandria CALLISTO spectrometer: First results," Advances in Space Research, vol. 72, no. 3, pp. 844-853, 2023, doi: 10.1016/j.asr.2022.06.054.

[3] O. Giersch, J. Kennewell, and M. Lynch, "Solar radio burst statistics and implications for space weather effects," Space Weather, vol. 15, no. 11, pp. 1511-1522, 2017, doi: 10.1002/2017SW001658.

[4] D. E. Gary, T. S. Bastian, and applications, "Solar Radio Burst Effects on Radio - and Radar - Based Systems," Space weather effects, pp. 141-152, 2021, doi: 10.1002/9781119815570.ch6.

[5] H. Salmane, R. Weber, K. Abed-Meraim, K.-L. Klein, X. Bonnin, and S. Climate, "A method for the automated detection of solar radio bursts in dynamic spectra," Journal of Space Weather, vol. 8, p. A43, 2018, doi: 10.1051/swsc/2018028.

[6] W. Yang, Z. W Zhen, M. Wang, et al. "A novel low frequency radio astronomical observation array(1~90 MHz) and its first light," Research in Astronomy and Astrophysics, vol 23:125007(9pp), 2023, doi:10.1088/1674-4527/acf6b1